CHAPTER 12

ESTIMATION OF STACKING FAULT ENERGY

CONTENTS

12.1 Introduction

Heidenreich and Shockley[1] emphasized the importance of stacking fault energy of face-centered cubic metals in determining the equilibrium ribbon width of extended dislocations, which makes it important in the theories of work hardening[2,3]. Further, as stacking fault energy is related to the difference in free energy between the hexagonal close packed structure and the face-centered cubic structure, it has a potential importance in the theory of alloy phases. In view of this importance there is always a need for finding the direct methods by which an estimation of stacking fault energy can be made.

In the past, stacking fault energies have been deduced from the energy of a coherent twin boundary[4] (on the assumption that the stacking fault energy is twice the twin boundary energy) and also from the temperature dependence of the stress strain curves[5]. Unfortunately, all these results depend upon the validity of theories still held in question and the stacking fault energy tends to appear simply as yet another adjustable parameter in the theory rather than as an independently known quantity.

The effect of stacking faults on X-ray diffraction has been used as a mean:: of determining stacking fault densities, but since the theory applied is only to the faults of large area and the effect of stacking fault ribbons is unknown, the interpretation of the results in terms of stacking fault energy[6] has only a qualitative significance.

The application of transmission electron microscopy to the study of dislocations in thin foils has made it possible to observe partial dislocations in a ribbon. It is now possible to get a detailed knowledge concerning the partial dislocations and the stacking faults. In particular, a number of methods have been developed for estimating the stacking

fault energies from the geometrical configurations of partial dislocations. A brief discussion of these methods will be given below and the formulas thus obtained will be used for the measurement of stacking fault energies in TaS_2 crystals described in this chapter.

12.2 Methods of Estimating Stacking Fault Energy

12.2.1 Extended nodes

Since in the lattices having a layered structure the nodes are situated in the plane of the foil and the stacking fault energies are small, the faults are wide and therefore it is easy to make accurate measurements of their geometry.

If we neglect the interaction with the other partials of the extended node, as would be the case in very wide nodes, one gets a very simple relation for γ as

$$\gamma = \frac{\mu b^2}{2\pi R} \quad .. \quad .. \quad 12.1$$

Here R is the radius of curvature of the extended node, μ is the shear modulus and b is the Burgers vector. This relation expresses the equilibrium

curvature of a dislocation under the constant shear stress of the stacking fault. The gain in energy due to the reduction of the stacking fault area is compensated by the increase in energy due to the lengthening of the dislocation.

Since this formula does not take into account either the character of the ribbon or the interaction with the other partials, it only gives an approximate estimation of the stacking fault energy. However, in order to minimize these effects and the effects of external stresses on the node, measurements for R were confined to nodes which were reasonably symmetrical and which were not too close to other dislocations.

12.2.2 Isolated two-fold ribbons

There has been some controversy over whether or not dislocations and dislocation nodes in silicon are dissociated into shockly partial dislocations. The early observations[7] showed that dislocation nodes in silicon were appreciably extended. These observations were criticised by Booker and Brown[8], who pointed out that unextended nodes could appear extended, under certain diffracting conditions, and that the 'partials'

in the image of Aerts et al[7] did not cross over between the nodes. Computations by Shaw and Brown[9] showed that dislocation nodes with a width less than 1/2 ξ_g could not be distinguished from unextended nodes in strong beam images.

Actually some doubt always remained whether or not dislocations in Si and Ge were dissociated at all[10]. This question was unambiguously resolved by Ray and Cockayne[11] who using weak beam technique, directly observed dislocations split into partials in Si, subsequently, similar observations were reported in Ge[12,13]. The author has used this versatile technique of weak beam to observe the isolated dissociated two-fold ribbons in TaS_2.

The value of the separation of the partials of an edge dislocation can be used to estimate the stacking fault energy γ. By applying isotropic theory in an infinite crystal the stacking fault energy follows from

$$\gamma = \frac{\mu b^2}{8\pi d_0} \left[\frac{2-\nu}{1-\nu}\right] \quad .. \quad 12.2$$

where d_0 expresses the equilibrium separation of the partial. d_0 is calculated from the formula,

$$d = d_0 \left\{ 1 - \left[2\nu / (2 - \nu) \right] \cos 2\phi \right\} \quad 12.3$$

d = distance between partials in a ribbon,

b = Burgers vector of the partial,

ϕ = angle between the total Burgers vector and ribbon,

μ = shear modulus and

ν = Poisson's ratio.

12.2.3 Three-fold ribbons

If the three partials comprising the three-fold ribbons go out of contrast simultaneously, indicating that their Burgers vectors are the same, then such symmetrical ribbons canbe used to estimate the stacking fault energy using the method outlined by Amelinckx and Delavignette[14]. According to them for ribbons, consisting of three partials with the same Burgers vectors

$$\gamma_1 = A \left(\frac{1}{x} + \frac{1}{x+y} \right)$$

and

$$\gamma_2 = A \left(\frac{1}{y} + \frac{1}{x+y} \right) \quad .. \quad 12.4$$

where $A = \beta \cos^2 \phi + \alpha \sin^2 \phi$

$$\beta = \frac{\mu b^2}{2\pi}$$

$$\alpha = \frac{\mu b^2}{2(1-\nu)}$$

x and y are the widths of the ribbons, γ_1 and γ_2 are the stacking fault energies in the regions x and y respectively, b is the Burgers vector, ν is the Poisson ratio, μ is the shear modulus, ϕ is the angle made by the Burgers vector with the partials.

12.3 Observations and Discussion

12.3.1 Extended nodes

For an accurate estimation of stacking fault energy, it is advisible to use only those nodes which are relatively free from interaction with the other dislocations. Regions showing isolated nodes were, therefore, selected and the bright field picture and the weak beam picture of an isolated node, so taken, is shown in Figs. 12.1(a) and 12.1(b) respectively. The boundaries of the partials forming the nodes are clearly seen in Fig. 12.1(b). The radii of curvature

of this node are used to determine the stacking fault energy by using the relation,

$$\gamma = \frac{\mu b^2}{2R},$$

obtained in the earlier section. Since μ for TaS_2 is not known, only the ratio γ/μ which is proportional to stacking fault energy alone was estimated to be 20.181×10^{-12} cm.

The relation $\gamma = \frac{\mu b^2}{2R}$, however does not take into account the interaction between the partials forming the node and it is therefore only a rough approximation.

Siems et al.[15] have indicated a better procedure to obtain stacking fault energy from extended nodes. The interaction between the partials is taken into account to a certain extent and the total energy is minimized by means of variational procedure. The specific stacking fault energy is then given by

$$\gamma = K\psi_0 / y_0\sqrt{3} \qquad 12.5$$

where $K = \frac{\mu b^2}{8\pi} \cdot \frac{2+\nu}{1+\nu}$ for edge ribbons

and $K = \frac{\mu b^2}{8\pi} \cdot \frac{2-3\nu}{1-\nu}$ for screw ribbons

ψ_0 is a dimensionless number which is equal to 3.85 for an edge ribbon and 4.37 for a screw ribbon. The meaning of y_0 is clear from Fig. 12.1(c). Using this method the value of γ_1/μ and γ_2/μ obtained for edge ribbon and for a screw ribbon come out to be 69.288×10^{-12} and 35.93×10^{-12} cm. respectively.

12.3.2 Two-fold ribbons

During the course of present investigation the author has come across the isolated dissociated two-fold ribbons in TaS_2. A striking example of this is shown in Fig. 12.2, which is a high resolution $(1\bar{2}0)$ weak beam dark field micrograph of a dislocation with Burgers vector $(1\bar{1}0)$ with $s(\bar{1}20)$, showing two peaks in the image with a separation of about 48 Å. Also shown in Fig. 12.2 is the selected area diffraction pattern from the area imaged showing the weak $(1\bar{2}0)$ reflection and strong $(\bar{1}20)$ reflection.

The value of separation of the partials of an edge dislocation was used to estimate the stacking fault energy γ by using the expression 12.2. Since

μ for TaS_2 is not known, only the ratio γ/μ which is proportional to the stacking fault energy can be calculated.

Substituting the measured values of separation of the partials, angle between the Burgers vector of the dislocations and the direction of the ribbons and other known values for TaS_2 the value of γ/μ as determined comes out to be 54.56×10^{12} cm.

12.3.3 Three-fold ribbons

During the course of investigation author came across striking observations of multiple ribbons in WSe_2 which could be used for the calculations of the stacking fault energy.

A representative example of three-fold ribbons observed in some of the specimens of WSe_2 crystals is shown in Fig. 12.3. It was seen that the three partials comprising the three-fold ribbons go out of contrast simultaneously, proving that their Burgers vectors are the same. The ribbon widths x and y shown in Fig. 12.3 are used to calculate the stacking fault energy using the [illegible] relation 12.4. Since μ for WSe_2 is not known, only the ratio γ_1/μ and γ_2/μ which are proportional to stacking fault energy can

only be estimated.

For actual measurements the region shown in Fig. 12.3(a) was photographed in weak beam (Fig. 12.3(b), and the computation of γ_1/μ and γ_2/μ have been made on the ribbons shown in this figure.

Using the values of x and y from Fig. 12.3(b) γ_1/μ and γ_2/μ have been estimated as 52.27×10^{-12} cm and 46.11×10^{-12} cm. respectively.

Since we have in our microscope a built in facility for varying the temperature of the specimens, a region showing three-fold ribbons (Fig.12.4 (a)) at - 164° C was heated up to 46° C (Fig. 12.4(b)). A comparison of the two figures clearly reveals that the width of the partials forming the three fold ribbons marked XX in Fig. 12.4(a) has considerably increased.

As before computations of γ_1/μ and γ_2/μ were made from the width of the ribbons in Fig. 12.4(a). Region shown in Fig. 12.4(a) was heated at different temperatures. Sufficient time being given at each temperature for its stabilization. γ_1/μ and γ_2/μ were computed fromthe width of the ribbons at each stage. These values have been computed in Table 12.1. A plot showing the variation of γ_1/μ and γ_2/μ

Table 12.1

Variation of γ/μ with temperature

Temperature in ^{o}K	$\frac{\gamma_1}{\mu} \times 10^{12}$ cm	$\frac{\gamma_2}{\mu} \times 10^{-12}$ cm
109	34.872	37.455
169	45.640	47.427
260	41.400	44.413
278.5	39.184	42.081
299	34.659	37.898
319	31.937	34.666

with temperature is shown in Fig. 12.5.

It is clearly seen from the figure that the stacking fault energy decreases as the temperature is increased. Similar observations have also been reported in silver[16] and graphite. In the case of silver these results were inferred directly from the measurements of the radii of the extended nodes in silver foils thinned from bulk and measurements were reported at 295° K and 600° K, while in the case of graphite the results were estimated from the width of isolated ribbons at different temperatures.

12.4 Conclusions

1. The values of $\sqrt{/\mu}$ as determined for TaS_2 crystals using extended nodes come out to be 69.288×10^{-12} cm. (edge ribbon) and 35.93×10^{-12} cm (screw ribbon).
2. "$\sqrt{/\mu}$" obtained from isolated two-fold ribbons in TaS_2 was determined to be 54.56×10^{-12} cm.
3. Three-fold ribbons in WSe_2 single crystals yielded the values of $\sqrt{_1/\mu}$ and $\sqrt{_2/\mu}$ as 52.27×10^{-12} cm and 46.11×10^{-12} cm respectively.

4. The small value of stacking fault energy suggests the possibility of a profuse polytypism in these crystals.

12.5 References

1. Heidenreich, R. D. and Shockley W. Report of a conference on Strength of solids (The Physical Society of London) (1948) 57.

2. Seeger, A. "Dislocations and Mechanical properties of Crystals" (Wiley International, New York) (1956).

3. Hirsch, P. B. J. Inst. Metals, 87 (1959) 406.

4. Fullman, R. L. J. Appl. Phys. 22 (1950) 448.

5. Seeger, A., Berner, R. and Wolf, W. Z. Phys. 155 (1959) 247.

6. Christian, J. W. and Supreadbereugh, J. Proc. Phys. Soc. (London) B 70 (1957) 1151.

7. Aerts, E., Delavignette, P., Siems, R. and Amelinckx, S. J. Appl. Phys. 33 (1962) 3078.

8. Booker, G. R. and Brown, L. M. Phil. Mag. 11 (1965) 1315.

9. Shaw, A. M. B. and Brown, L. M. Phil. Mag. 15 (1967)797.

10. Haasen, P. and Schroter, W.
"Fundamental Aspects of Dislocation Theory" (Ed. by Simmons, J. A., Dewit, R. and Bullough, R) Special publication 317 , 2 (U.S. National Bureau of Standards) 1231.

11. Ray, I. L. F. and Cockayne, D. J. H.
Proc. Roy. Soc. A 325 (1971) 543.

12. Ray, I. L. F. and Cockayne, D. J. H.
Microscope 98 (1973) 170.

13. Haussermann, F. and Schaumberg, H.
Phil. Mag. 27 (1973) 745.

14. Amelinckx, S. and Delavignette, P.
"Imperfections in Crystals"
(1962) 295.

15. Siems, R., Delavignette, P. and Amelinckx, S.
Z. Phys. 161 (1961) 502.

16. Schwab, S.
J. of Appl. Phys. 37 (1966) 4275.

Captions of the figures

Fig. 12.1(a)	Bright field picture of an isolated extended node.
Fig. 12.1(b)	Corresponding weak beam picture of Fig. 12.1(a).
Fig. 12.1(c)	Schematic view of extended node in order to illustrate the notations used.
Fig. 12.2	Weak beam dark field picture of two-fold ribbon.
Fig. 12.3(a)	Bright field electron micrograph showing three-fold ribbons in WSe_2 crystals.
Fig. 12.3(b)	Weak beam dark field electron micrograph of Fig. 12.3(a).
Fig. 12.4(a)	A region showing three-fold ribbons at $-164^{\circ}C$.
Fig. 12.4(b)	Same region as Fig. 12.4(a) at $+46^{\circ}$ C.
Fig. 12.5	Plots showing variation of γ_1/μ and γ_2/μ with temperature.

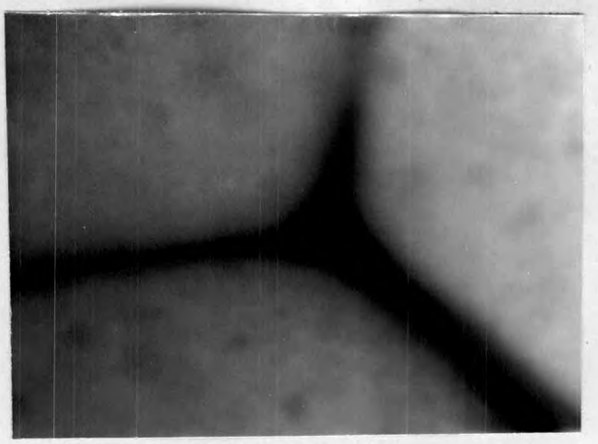

Fig. 12.1(a) X 174,000

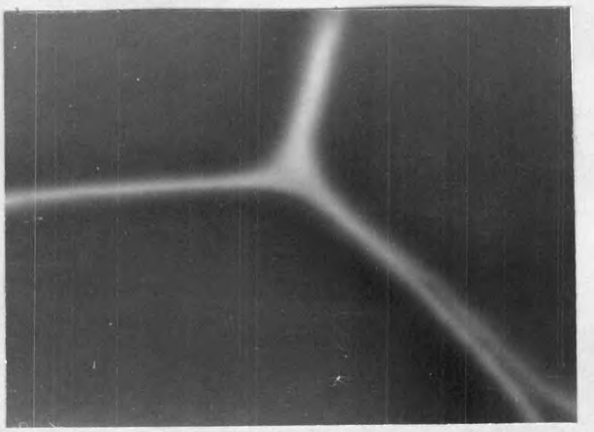

Fig. 12.1(b) X 174,000

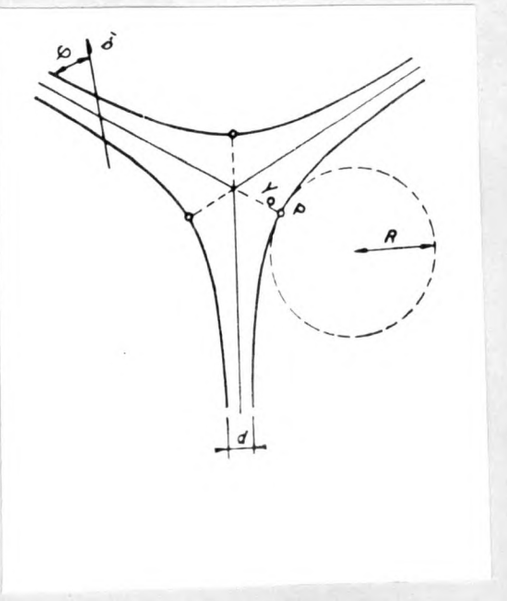

Fig. 12.1(c)

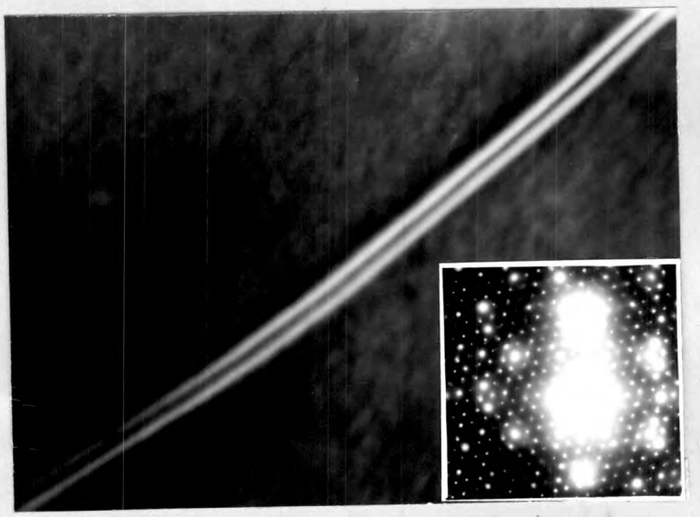

Fig. 12.2 X 186,000

Fig.12.3(a) X 121,500

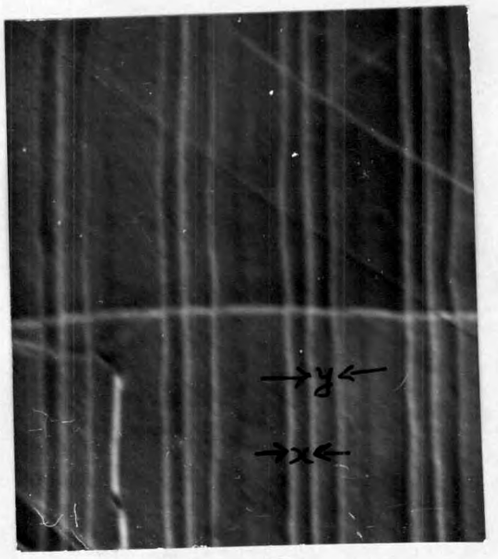

Fig.12.3(b) X 121,500

Fig.12.4(a) X 180,000

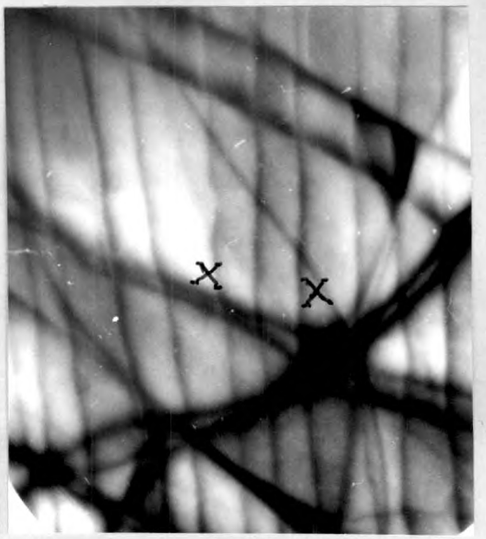

Fig. 12.4(b) X 180,000

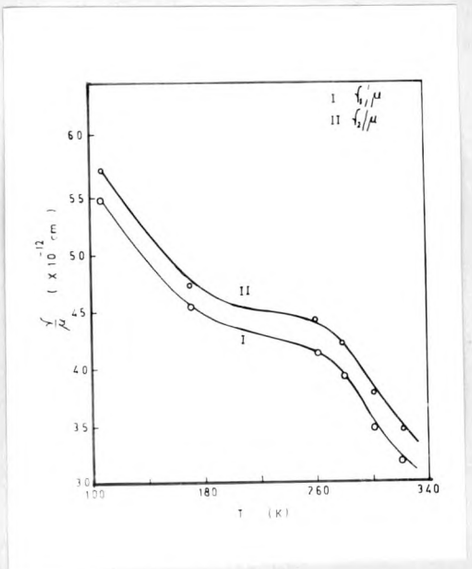

Fig. 12.5